

1 **Title: Sources and upstream pathways of the densest overflow water in the Nordic Seas**

2

3 **Authors:** Jie Huang^{1,2,*}, Robert S. Pickart², Rui Xin Huang², Peigen Lin², Ailin Brakstad³, and

4 Fanghua Xu¹

5

6 **Affiliations:**

7 ¹Ministry of Education Key Laboratory for Earth System Modeling, and Department of Earth
8 System Science, Tsinghua University, Beijing, China

9 ²Woods Hole Oceanographic Institution, Woods Hole, USA

10 ³Geophysical Institute, University of Bergen, and Bjerknes Centre for Climate Research, Bergen,
11 Norway

12

13 *Corresponding author: huangj15@mails.tsinghua.edu.cn

14

15

December 2019

16

Submitted to *Nature Geoscience*

17 **The overflow water from the Nordic Seas comprises the deepest limb of the Atlantic**
18 **Meridional Overturning Circulation, yet questions remain as to where it is ventilated and**
19 **how it progresses to the Greenland-Scotland Ridge. Here we use historical hydrographic**
20 **data from 2005-2015, together with satellite altimeter data, to elucidate the source regions of**
21 **the Denmark Strait and Faroe Bank Channel overflows and the pathways by which the dense**
22 **water reaches the respective sills. A recently-developed metric is used to calculate how close**
23 **two water parcels are to each other in terms of physical properties, based on potential density**
24 **and potential spicity. This reveals that the Greenland Sea gyre is the primary wintertime**
25 **source region for the densest portion of both overflows. After subducting, the water**
26 **progresses southward along several ridge systems towards the Greenland-Scotland Ridge.**
27 **These inferred flow paths are confirmed using absolutely-referenced circulation maps.**
28 **Extending the calculation back to the 1980s reveals that the ventilation occurred previously**
29 **along the periphery of the Greenland Sea gyre, but that the pathways to the south remained**
30 **the same.**

31 **1. Introduction**

32 The overflows from the Nordic Seas feed the lower limb of the Atlantic Meridional
33 Overturning Circulation (AMOC), which helps regulate Earth's climate. There are two general
34 classes of overflow water¹: (1) "Atlantic-origin" overflow water which is formed by strong air-sea
35 heat loss along the rim current system of the Nordic Seas²; and (2) "Arctic-origin" overflow water
36 which stems from the interior basins of the western Nordic Seas where water mass transformation
37 takes place via open-ocean convection³. The East Greenland Current (EGC) transports Atlantic-
38 origin water to Denmark Strait, while the North Icelandic Jet (NIJ) advects a comparable amount
39 of the denser Arctic-origin water to the strait^{3,4,5} (Fig. 1). The leading hypothesis is that the NIJ

40 sources from the Iceland Sea, as the lower limb of a local overturning cell³. Both types of overflow
41 water also enter the North Atlantic through the Faroe Bank Channel^{6,7}. Previous studies suggest
42 that the deep water formed in the Greenland Sea, and a local overturning loop within the
43 Norwegian Sea, supply this overflow^{8,9}. To date, however, consensus has not been reached
44 regarding the origin and upstream pathways of the densest component of the overflow water, which
45 ventilates the deepest layers of the North Atlantic.

46 Water denser than 27.8 kg m^{-3} (potential density referenced to the sea surface, σ_0) is generally
47 identified as overflow water¹⁰. The Arctic-origin overflow, found in the deepest part of Denmark
48 Strait and the Faroe Bank Channel, is characterized by $\sigma_0 \geq 28.03 \text{ kg m}^{-3}$ and θ (potential
49 temperature) $\leq 0 \text{ }^\circ\text{C}$ ^{3,11}. Using data from a large number of shipboard surveys, an Arctic-origin
50 overflow transport mode of the NIJ was identified, where the bulk of the transport is confined to a
51 small region in potential temperature-salinity (θ - S) space⁵. This mode is centered near $-0.27 \text{ }^\circ\text{C}$ in
52 potential temperature and 34.91 in practical salinity, corresponding to $\sigma_0 = 28.05 \text{ kg m}^{-3}$ and
53 accounting for 26% of the total overflow transport⁵. By comparison, at the Faroe Bank Channel
54 sill the densest component ($\theta \leq 0 \text{ }^\circ\text{C}$) contributes to more than half of the total overflow transport¹¹.
55 This component has almost the same properties ($\bar{\sigma}_0 = 28.05 \text{ kg m}^{-3}$, $\bar{\theta} = -0.4 \text{ }^\circ\text{C}$ and $\bar{S} = 34.91$) as
56 the transport mode of the NIJ. The similarity of the hydrographic properties of these two dense
57 modes suggests a common source.

58 **2. Applying a new metric to trace the source of the densest overflow water**

59 We use a comprehensive historical hydrographic dataset of the Nordic Seas, described in the
60 Methods section, to elucidate the source regions and pathways of the Arctic-origin overflow water
61 feeding Denmark Strait and the Faroe Bank Channel. A recently-developed metric, referred to as

62 the σ_0 - π_0 distance, is used to calculate how close two different water parcels are to each other in
63 terms of physical properties, where σ_0 is potential density and π_0 is potential spicity¹². The metric
64 is effective because the isolines of potential density are orthogonal to the isolines of potential
65 spicity, and their gradients have the same magnitude (see the Methods section). The Arctic-origin
66 overflow water is defined by the transport mode of the NIJ in σ_0 - π_0 space, $\sigma_0 = 28.05 \text{ kg m}^{-3}$ and
67 $\pi_0 = -3.11 \text{ kg m}^{-3}$ (the results are nearly indistinguishable using the σ_0 - π_0 values of the densest
68 Faroe Bank Channel overflow water). Computationally, we calculate the σ_0 - π_0 distance between
69 the water parcels in question upstream of the Greenland-Scotland Ridge and the NIJ transport
70 mode. We consider the time period 2005-2015 to avoid effects of decadal variability, which are
71 addressed in the last section of the paper.

72 We begin by asking, where in the Nordic Seas are the late-winter surface properties most
73 closely aligned with the Arctic-origin overflow water? To answer this we determined the mixed-
74 layer characteristics (temperature, salinity, density and depth) for approximately 8600 late-winter
75 (February to April) profiles, using a multi-step procedure¹³. Not surprisingly, the deepest and
76 densest mixed layers are found within the Greenland Sea gyre due to the strong atmospheric
77 forcing and weak stratification there^{14,15} (Supplementary Fig. 1). The Iceland Sea gyre also stands
78 out as a region of deep, dense mixed layers, but to a lesser extent than the Greenland Sea. Notably,
79 the smallest σ_0 - π_0 distances associated with the mixed layers (as small as 0.005 kg m^{-3}) are found
80 in the Greenland Sea (Fig. 2a), indicating that this is the major source region of the densest
81 overflow water entering the North Atlantic. A second region of relatively small σ_0 - π_0 distances
82 occurs in the northwest portion of the Iceland Sea, consistent with the notion that this region can
83 supply some of the Arctic-origin overflow water to the NIJ^{16,17}. Our results imply, however, that
84 the Iceland Sea source is relatively minor (Fig. 2a).

85 To elucidate the connection between the formation region of the Arctic-origin overflow and
86 the presence of this water in Denmark Strait and the Faroe Bank Channel, we calculated the σ_0 - π_0
87 distances at different depth horizons in the Nordic Seas using the year-round hydrographic profiles.
88 This reveals where the water is present after late-winter subduction. Fig. 2b shows the σ_0 - π_0
89 distance distribution between 250-300 m, which is the depth range of the maximum velocity in the
90 NIJ¹⁸. The smallest σ_0 - π_0 distances still occur in the Greenland Sea. However, a potential pathway
91 of the Arctic-origin overflow water emerges from this map. In particular, small σ_0 - π_0 distances
92 stem southward from the Greenland Sea along the Mohn Ridge, across the West Jan Mayen Ridge
93 into the Iceland Sea, then along the Kolbeinsey Ridge – ultimately progressing into Denmark Strait
94 via the NIJ. Note that no small σ_0 - π_0 distances are found along the slope of Greenland, confirming
95 that Arctic-origin overflow water is not advected by the East Greenland Current in this depth range.

96 The lateral distribution of σ_0 - π_0 distances in the 600-650 m layer, near the sill depth of
97 Denmark Strait, is generally consistent with the shallower layer (Fig. 2c). However, there are two
98 notable differences. First, small σ_0 - π_0 distances now extend eastward along the northern slope of
99 the Iceland-Faroe Ridge into the Faroe Bank Channel. Second, there are two bands of small values
100 on either side of the Iceland Sea: one along the eastern side of the Kolbeinsey Ridge (similar to
101 that seen in the shallower layer), and the other along the Jan Mayen Ridge. This suggests that, at
102 this deeper depth horizon, two potential pathways exist carrying Arctic-origin overflow water from
103 the Greenland Sea to the Faroe Bank Channel along the north-south ridges bounding the Iceland
104 Sea. The σ_0 - π_0 distance map for the depth range of the Faroe Bank Channel sill (800-850 m) is
105 qualitatively similar to that in Fig. 2c. When using the Faroe Bank Channel transport mode instead
106 of the NIJ transport mode to compute the σ_0 - π_0 distances, the Jan Mayen Ridge pathway is even
107 more evident in this depth range (not shown).

108 As a metric of the vertical structure of the σ_0 - π_0 distances, in Fig. 2d we plot the shallowest
109 depth at which the value equals 0.05 kg m^{-3} (which is the threshold used in Figs. 2a-c to define
110 small σ_0 - π_0 distances). This map also reveals the pathways discussed above for Arctic-origin
111 water to progress from the Greenland Sea gyre to the two overflows. Interestingly, it implies as
112 well that the small σ_0 - π_0 distance signal stays at roughly the same depth approaching Denmark
113 Strait in the NIJ, but that it deepens approaching the Faroe Bank Channel along the Iceland-Faroe
114 Ridge. Also in Fig. 2d one sees that the shallowest depth of small σ_0 - π_0 distances along the east
115 coast of Greenland is deeper than the sill depth of Denmark Strait (650 m). This implies that the
116 Arctic-origin water located below the Atlantic-origin water in the EGC is too deep to contribute to
117 the densest Denmark Strait overflow. However, there is evidence of aspiration of Arctic-origin
118 water just upstream of the sill¹⁹.

119 **3. Upstream overflow pathways derived from composite sections**

120 The distributions of σ_0 - π_0 distances presented above suggest that the Arctic-origin overflow
121 water crossing the Greenland-Scotland Ridge at Denmark Strait and the Faroe Bank Channel
122 originates primarily from the Greenland Sea, and that there are topographically-steered pathways
123 by which the water progresses from the Greenland Sea gyre to the vicinity of the ridge. We now
124 present kinematic evidence of these pathways using the historical hydrographic data in conjunction
125 with satellite absolute dynamic topography data. We focus on five composite sections (Fig. 3a)
126 that cross the ridge systems as well as the Iceland and Greenland Sea gyres, chosen to resolve the
127 circulation in question.

128 Relative geostrophic velocities are computed using the hydrographic data, then referenced
129 using the mean gridded surface geostrophic velocity field obtained from satellite altimeter data

130 (see the Methods section). The surface geostrophic vectors show the major currents in the study
131 region (Fig. 3b). The two branches of the Norwegian Atlantic Current (NAC) flow northward, with
132 the western branch turning to the northeast along the Mohn Ridge on the eastern side of the
133 Greenland Sea gyre. The southward-flowing EGC is evident, as is the North Icelandic Irminger
134 Current (NIIC) flowing around the north side of Iceland. There is relatively little surface signature
135 of the Greenland Sea gyre nor the Iceland Sea gyre.

136 The first two composite sections (S1 and S2) reveal the cold near-surface water in the center
137 of the Greenland Sea gyre (Fig. 3c and d). The strongly sloped isopycnals on the western side are
138 associated with the EGC, while those on the eastern side are associated with the NAC. The flat
139 isopycnals between the two fronts are consistent with the weak surface flow of the gyre. The third
140 composite section (S3) is south of the Greenland Sea gyre, but still shows the strong EGC and
141 NAC fronts. The last two composite sections (S4 and S5) pass through the northern and central
142 portions of the Iceland Sea gyre, respectively. Here the NAC front is not associated with the eastern
143 edge of the gyre, but is found farther to the east. However, the EGC abuts the western side of the
144 gyre, as it did for the Greenland Sea.

145 We present the calculated circulation at three depth horizons: the surface, 300 m, and 650 m
146 (Fig. 4). The latter two levels correspond to the σ_0 - π_0 distance maps in Fig. 2b and c, respectively.
147 At the surface (Fig. 4a) the warm NAC flows northward east of the Mohn Ridge (as was noted
148 earlier in Fig. 3b-d). The hydrographic front of the NAC is associated with strong thermal wind
149 shear, which is large enough to reverse the circulation at 300 m and deeper (sections S2 and S3 in
150 Fig. 4b and c). This provides a pathway of Arctic-origin overflow water away from the Greenland
151 Sea gyre that continues southward on eastern side of the Iceland Sea along the Jan Mayen Ridge
152 (sections S4 and S5 in Fig. 4b and c). The circulation maps also reveal a second dense water

153 pathway that emerges at section S2 west of the Mohn Ridge and strengthens by section S3. This
154 branch passes through the West Jan Mayen Ridge and flows southward in the Iceland Sea on the
155 eastern side of the Kolbeinsey Ridge (sections S4 and S5, Fig. 4b and c). Overall, these circulation
156 pathways are consistent with the σ_0 - π_0 distance distributions presented above, including the two
157 bands of low σ_0 - π_0 distance on the two sides of the Iceland Sea (Fig. 2c).

158 The two branches of Arctic-origin overflow water emanating from the vicinity of the Mohn
159 Ridge appear to be dynamically distinct. The western branch is nearly barotropic, with a signature
160 at the sea surface starting at section S3 (Fig. 4a and supplementary Fig. 3). In contrast, the eastern
161 branch is sub-surface intensified with stronger flow at 650 m (Fig. 4c and supplementary Fig. 3).
162 The fate of these two branches remains to be determined. Previous mooring data have suggested
163 the presence of a bottom intensified current progressing eastward along the Iceland-Faroe Ridge,
164 presumably supplying the Faroe Bank Channel overflow²⁰. It is likely that the two branches of
165 Arctic-origin overflow water identified here feed both the NIJ and this current, but the precise
166 partitioning and manner in which this happens needs to be worked out. Notably, the suggested
167 pathways presented here are consistent with a two-layer modeling study²¹ and a tracer release
168 experiment²².

169 **4. Long-term variation in the source of the densest overflow water**

170 We now consider the complete time period of the historical hydrographic observations to
171 address long-term differences in the source of the Arctic-origin overflow water to the Greenland-
172 Scotland Ridge. We focus on the densest overflow water ($28.03 \leq \sigma_0 \leq 28.06 \text{ kg m}^{-3}$, $\theta \leq 0 \text{ }^\circ\text{C}$, and
173 depth $\leq 850\text{m}$) in four geographical regions: the Greenland Sea gyre water (GSW), Mohn Ridge
174 water (MRW), North Iceland slope water (ISW), and East Faroes water (EFW). These four regions

175 are outlined in Figure 5b. The characteristics of the NIJ water have varied by more than 0.3 °C in
176 temperature and 0.02 in salinity from 1990 to the present¹⁷. Here we use the densest ISW water as
177 a proxy for the time-varying NIJ transport mode; in particular, a 3-year running mean of the
178 corresponding hydrographic properties within the ISW box over the 30-year hydrographic record
179 (1986-2015). The equivalent timeseries for the EFW box is used for the Faroe Bank Channel
180 transport mode (unsurprisingly, the two curves are very similar). Following this, we constructed
181 timeseries of σ_0 - π_0 distances between the GSW and the two transport modes, as well as the MRW
182 and the two modes (Fig. 5a). This reveals a marked increase in σ_0 - π_0 distance between the water
183 in the center of the Greenland Sea gyre and the water feeding the two overflows prior to 2007. In
184 contrast, the MRW has remained very close in hydrographic characteristics to the two transport
185 modes (Fig. 5a).

186 This result suggests that there has been a shift in the origin of the densest water feeding the
187 overflows, from the periphery of the Greenland Sea gyre to its center, after 2007. This is supported
188 by the lateral map of σ_0 - π_0 distances in the 600-650 m layer from 1986-2004, i.e. prior to the time
189 period considered in the above analysis (2005-15) (compare Fig. 5b to 2c). During both time
190 periods, however, the pathways of small σ_0 - π_0 distances remain the same: from the Mohn Ridge
191 into the Iceland Sea, then along the Jan Mayen and Kolbeinsey Ridges on the eastern and western
192 sides of the Iceland Sea, respectively. The earlier period map suggests a contribution to the Faroe
193 Bank Channel overflow from the southern half of the Norwegian Basin as well.

194 Why was the Greenland Sea gyre not the primary dense water source during the early time
195 period? This is due to the change in convection within the gyre over the 30-year record. The
196 vertical distribution of σ_0 - π_0 distance in the GSW box (Fig. 5c) shows values $< 0.05 \text{ kg m}^{-3}$
197 spanning the top 1000 m starting around 2007 (with small values extending to the surface

198 seasonally in winter). This is associated with warming of the ventilated water in the gyre due to
199 the weakening of deep convection, and salinification of the inflowing Atlantic water into the
200 Nordic Seas^{15,23}. Prior to 2007, the dense wintertime product in the center of the gyre was too cold
201 and fresh to match closely the properties of the two overflow transport modes. This change in
202 source region from outside the gyre to within the gyre likely has ramifications regarding the
203 dynamical processes and timescale for newly ventilated water to progress from the formation
204 region to the pathways supplying the overflows.

205 **5. Implications and Remaining Questions**

206 In this study we have elucidated the source and upstream pathways of the densest Arctic-origin
207 water supplying the Denmark Strait and Faroe Bank Channel overflows, using a new metric for
208 determining how close water parcels are to each other in terms of hydrographic properties. The
209 inferred pathways were confirmed using absolutely-referenced circulation maps. Our results
210 establish the Greenland Sea as the primary region of ventilation for the deepest layers of the North
211 Atlantic, and reveal the importance of topographically steered pathways in channeling the dense
212 water towards the Greenland-Scotland Ridge. This puts us in a position to understand better the
213 link between atmospheric forcing and the densest component of the AMOC, and how this might
214 be impacted by ongoing changes in the climate of the high latitude North Atlantic. Our study also
215 raises several new questions, including: How and why does the newly-convected water enter the
216 deep Mohn Ridge boundary current system after it is subducted? And how does this dense water
217 subsequently pass through the West Jan Mayen Ridge into the Iceland Sea? Finally, it remains
218 unknown how the dense Arctic-origin water ultimately feeds the westward-flowing NIJ and
219 eastward-flowing current along the Iceland-Faroe Ridge. These questions need to be addressed
220 with future observational and modeling studies.

221 **Methods**

222 The hydrographic data used in this study cover the time period 1986-2015 and the spatial
223 domain 59°-80°N and 30°W-20°E. The majority of the data were obtained from the Unified
224 Database for Arctic and Subarctic Hydrography (UDASH)²⁴. Additional data, particularly south
225 of 65°N which is outside the domain of UDASH, come from various archives as listed in
226 supplementary Table 1. All of the data were combined into a single hydrographic dataset, where
227 duplicates between the different archives were removed. In addition to the quality control already
228 performed on each data source, we required that all vertical profiles include both temperature and
229 salinity. We excluded measurements outside the expected range in the Nordic Seas [-2°C, 20°C]
230 and [20, 36] for potential temperature and practical salinity, respectively. Data with density
231 inversions exceeding 0.05 kg m⁻³ were also excluded, except when the inversion was associated
232 with a single data point, in which case the point in question was removed¹⁵.

233 A metric known as the σ_0 - π_0 distance is used to calculate how close two different water
234 parcels are to each other in terms of physical properties referenced at sea surface, where σ_0 is
235 potential density and π_0 is potential spicity¹². Contours of π_0 are orthogonal to those of σ_0 , hence
236 π_0 contains information regarding temperature and salinity not included in the potential density.
237 In contrast to θ - S space, the gradients in σ_0 - π_0 space are the same magnitude, allowing a
238 meaningful calculation of distance. The σ_0 - π_0 distance between the densest overflow water ($\sigma_{0,1}$,
239 $\pi_{0,1}$) and any upstream water parcel ($\sigma_{0,2}$, $\pi_{0,2}$) in the Nordic Seas is calculated by the following
240 equation:

$$241 \quad D_{1,2} = \sqrt{(\sigma_{0,1} - \sigma_{0,2})^2 + (\pi_{0,1} - \pi_{0,2})^2} .$$

242 The composite vertical sections were constructed using profiles from the historical

243 hydrographic dataset as follows. For each selected section, profiles with lateral distances less than
244 50 km from the line are used (grey crosses in Fig. 3a). The positions of profiles along the section
245 are determined by the distance between their projected location (black crosses in Fig. 3a) and the
246 location of the ridge (which is the origin of the section). The projected profiles are then gridded
247 using Laplacian-spline interpolation²⁵. The final gridded sections have a horizontal resolution of
248 25 km and a vertical resolution of 25 m. The relative geostrophic velocities normal to the sections
249 are calculated based on the gridded data. The absolute geostrophic velocities are obtained by using
250 satellite-derived mean surface geostrophic velocity from 2005 to 2015 as the reference, which can
251 be accessed at Copernicus Marine Environment Monitoring Service (CMEMS,
252 <http://marine.copernicus.eu>).

253

254 **Acknowledgements**

255 Funding for the study was provided by the US National Science Foundation under grants OCE-
256 1558742 (JH, RP) and OCE-1259618 (PL); the Bergen Research Foundation under grant
257 BFS2016REK01 (AB); and the National Natural Science Foundation of China No. 41576018 (FX)
258 and 41606020 (FX).

259

260 **Author contributions**

261 JH, RP, and AB assembled and analyzed the data; RH developed the σ_0 - π_0 distance methodology
262 and helped apply it; JH and RP wrote the paper and all authors interpreted the results and clarified
263 the implications.

264 **Competing interests**

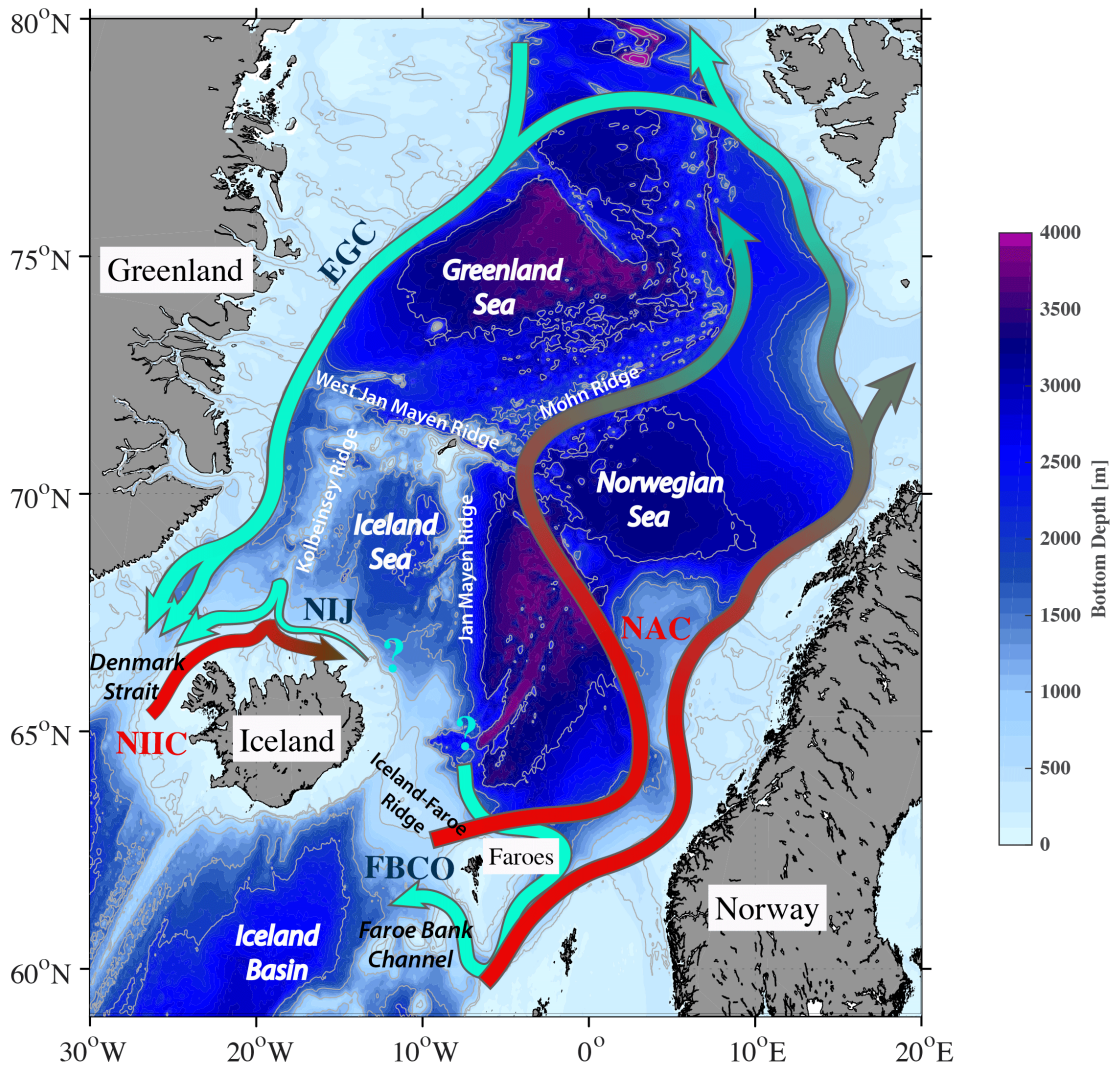
265 The authors declare no competing financial interests.

266 **References**

- 267 1. Hansen, B. & Østerhus S. North Atlantic–nordic Seas Exchanges, *Progress in oceanography*
268 **45(2)**, 109-208 (2000).
- 269 2. Mauritzen, C. Production of dense overflow waters feeding the North Atlantic across the
270 Greenland-Scotland Ridge. Part 1: Evidence for a revised circulation scheme, *Deep Sea*
271 *Research Part I: Oceanographic Research Papers* **43(6)**, 769-806 (1996).
- 272 3. Våge, K. *et al.* Significant role of the North Icelandic Jet in the formation of Denmark Strait
273 overflow water, *Nature Geoscience* **4(10)**, 723 (2011).
- 274 4. Mastropole, D. *et al.* On the hydrography of Denmark Strait, *Journal of Geophysical Research:*
275 *Oceans* **122(1)**, 306-321 (2017).
- 276 5. Semper, S. *et al.* The emergence of the North Icelandic Jet and its evolution from northeast
277 Iceland to Denmark Strait, *Journal of Physical Oceanography* **45**, 2499-2521 (2019).
- 278 6. Olsen, S. M., Hansen B., Quadfasel D. & Østerhus S. Observed and modelled stability of
279 overflow across the Greenland–Scotland ridge, *Nature* **455(7212)**, 519 (2008).
- 280 7. Østerhus, S., Sherwin T., Quadfasel D. & Hansen B. The overflow transport east of Iceland, in
281 *Arctic–Subarctic Ocean Fluxes*, edited, pp. 427-441, (Springer, Dordrecht, 2008).
- 282 8. Eldevik, T. *et al.* Observed sources and variability of Nordic seas overflow, *Nature Geoscience*
283 **2(6)**, 406 (2009).
- 284 9. Jeansson, E., Olsen A. & Jutterström S. Arctic Intermediate Water in the Nordic Seas, 1991-
285 2009, *Deep Sea Research Part I: Oceanographic Research Papers* **128**, 82-97 (2017).
- 286 10. Dickson, R. R. & Brown J. The production of North Atlantic Deep Water: Sources, rates and
287 pathways, *Journal of Geophysical Research* **C99**, 12319-12341 (1994).
- 288 11. Hansen, B. & Østerhus S. Faroe Bank Channel overflow 1995–2005, *Progress in*
289 *Oceanography* **75(4)**, 817-856 (2007).
- 290 12. Huang, R. X., Yu L. S. & Zhou S. Q. New definition of potential spicity by the least square
291 method, *Journal of Geophysical Research: Oceans* **123(10)**, 7351-7365 (2018).
- 292 13. Pickart, R. S., Torres D. J. & Clarke R. A. Hydrography of the Labrador Sea during active
293 convection, *Journal of Physical Oceanography* **32(2)**, 428-457 (2002).
- 294 14. Marshall, J. & Schoot F. Open-ocean convection: Observations, theory, and models. *Reviews*
295 *of Geophysics* **37**, 1-64 (1999).

- 296 15. Brakstad, A., Våge K., Håvik L. & Moore G. W. K. Water Mass Transformation in the
297 Greenland Sea during the Period 1986-2016, *Journal of Physical Oceanography* **49**, 121-140
298 (2019).
- 299 16. Våge, K., Moore G. W. K., Jónsson S. & Valdimarsson H. Water mass transformation in the
300 Iceland Sea, *Deep Sea Research Part I: Oceanographic Research Papers* **101**, 98-109 (2015).
- 301 17. Pickart, R. S. *et al.* The North Icelandic Jet and its relationship to the North Icelandic Irminger
302 Current, *Journal of Marine Research* **75(5)**, 605-639 (2017).
- 303 18. Huang, J. *et al.* Structure and Variability of the North Icelandic Jet From Two Years of Mooring
304 Data, *Journal of Geophysical Research: Oceans* **124**, 3987-4002 (2019).
- 305 19. Harden, B. *et al.* Upstream sources of the Denmark Strait Overflow: Observations from a high-
306 resolution mooring array, *Deep-Sea Research I* **112**, 94-112 (2016).
- 307 20. Hopkins, T.S., Baldasserini, G., Minnett, P., Povero, P. & Zanasca, P. Icelandic Current
308 Experiment. GIN SEA Cruise 88 - Data Report. Hydrography and Circulation. Tech. Rep.
309 SM-260, Saclant Undersea Research Centre (1992). URL
310 <https://openlibrary.cmre.nato.int/handle/20.500.12489/212>.
- 311 21. Yang, J. & Pratt L. J. Some dynamical constraints on upstream pathways of the Denmark Strait
312 Overflow, *Journal of Physical Oceanography* **44(12)**, 3033-3053 (2014).
- 313 22. Olsson, K. A. *et al.* Intermediate water from the Greenland Sea in the Faroe Bank Channel:
314 spreading of released sulphur hexafluoride, *Deep Sea Research Part I: Oceanographic*
315 *Research Papers* **52**, 279-294 (2004).
- 316 23. Lauvest, S. L. *et al.* Continued warming, salinification and oxygenation of the Greenland Sea
317 gyre. *Tellus* **70A**, 1-9 (2018).
- 318 24. Behrendt, A., Sumata H., Rabe B. & Schauer U. UDASH–Unified Database for Arctic and
319 Subarctic Hydrography, *Earth System Science Data* **10(2)**, 1119-1138 (2018).
- 320 25. Pickart, R. S. & Smethie W. M. Temporal evolution of the deep western boundary current
321 where it enters the sub-tropical domain, *Deep Sea Research Part I: Oceanographic Research*
322 *Papers* **45**, 1053-1083 (1998).

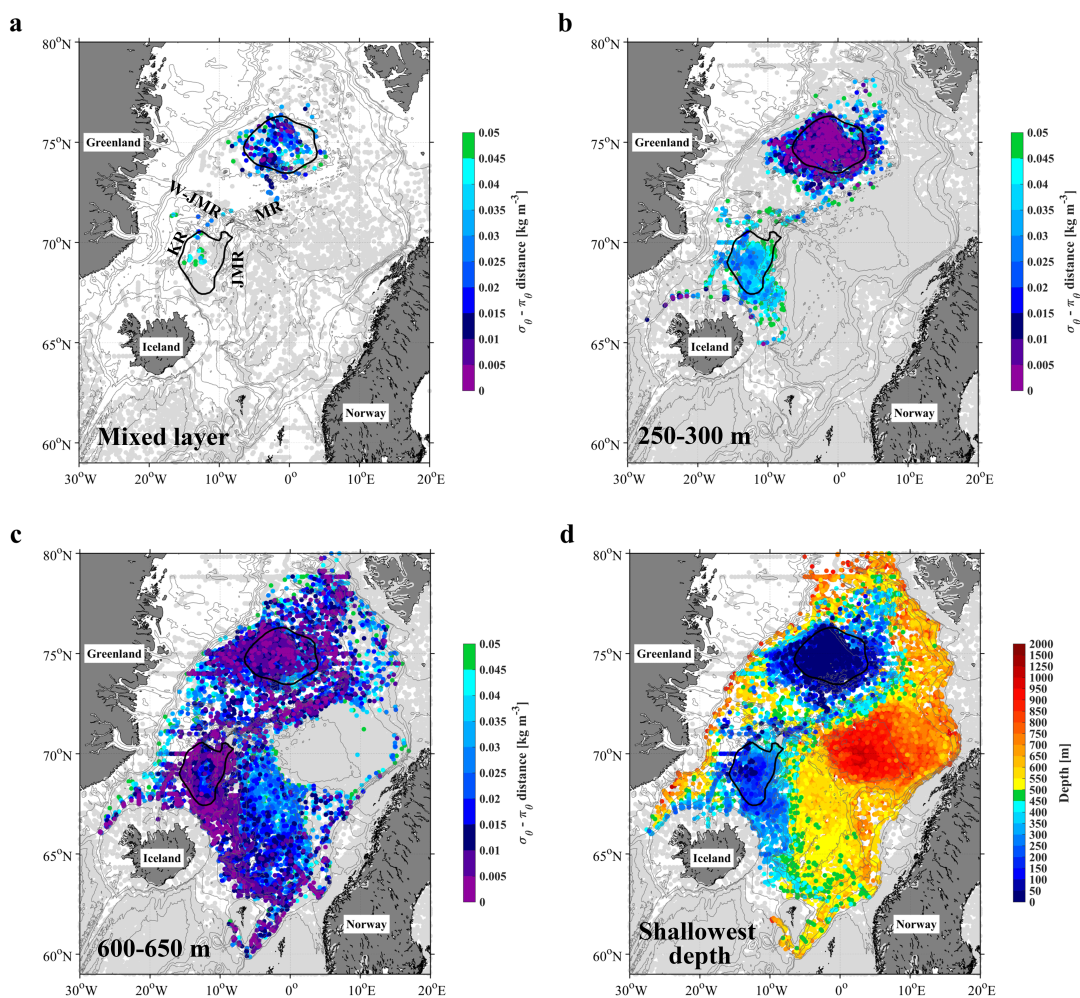
323



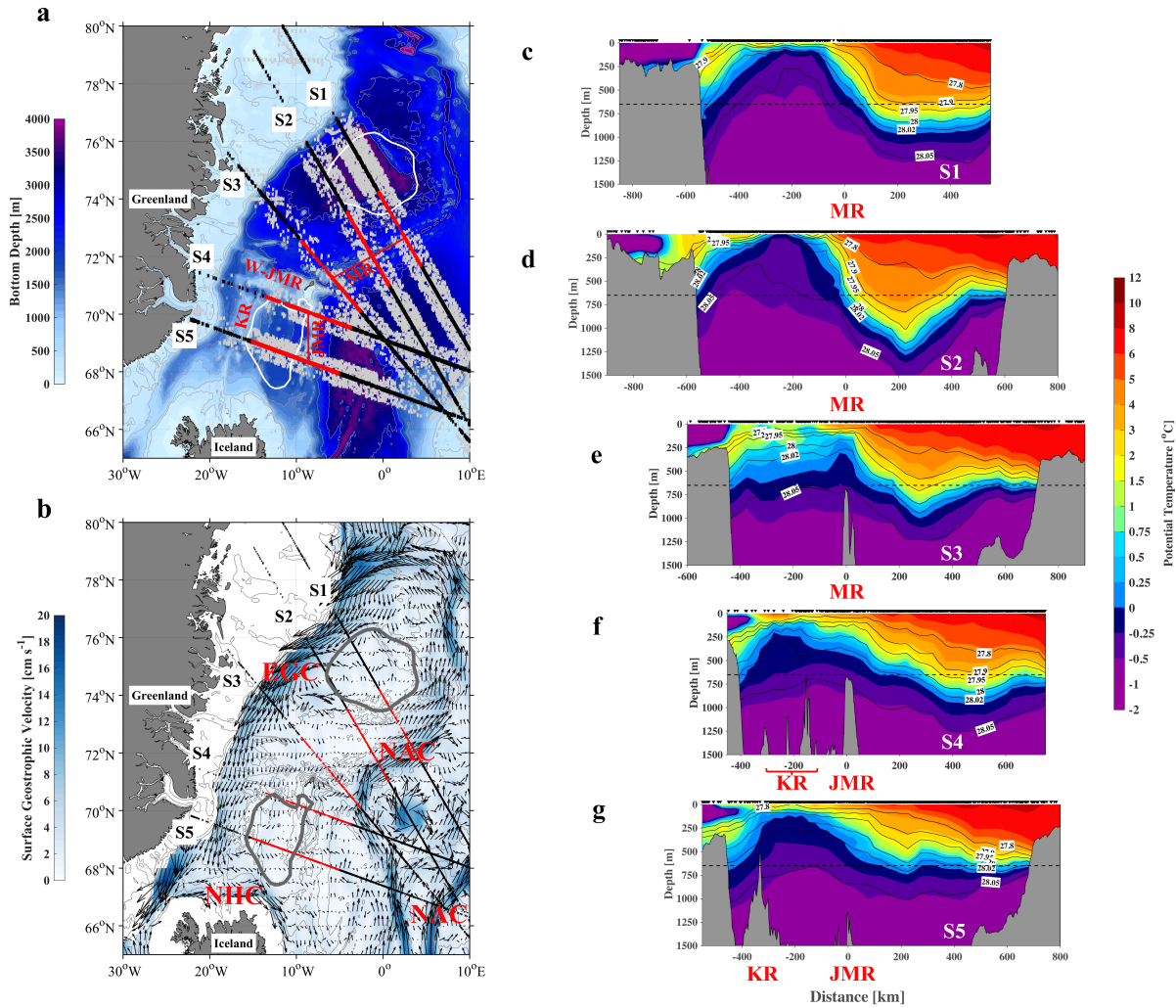
324

325 **Figure 1| Schematic circulation of the Nordic Seas.**

326 The pathways of warm Atlantic inflow and dense outflow are shown in red and green arrows,
 327 respectively. Colors and grey contours represent the bathymetry from ETOPO2, and the relevant
 328 ridges are named. The abbreviations are: NAC, Norwegian Atlantic Current; NIIC, North Icelandic
 329 Irminger Current; EGC, East Greenland Current; NIJ, North Icelandic Jet; FBCO, Faroe Bank
 330 Channel overflow. Question marks denote uncertainty in upstream the source/pathways of the
 331 dense overflows.



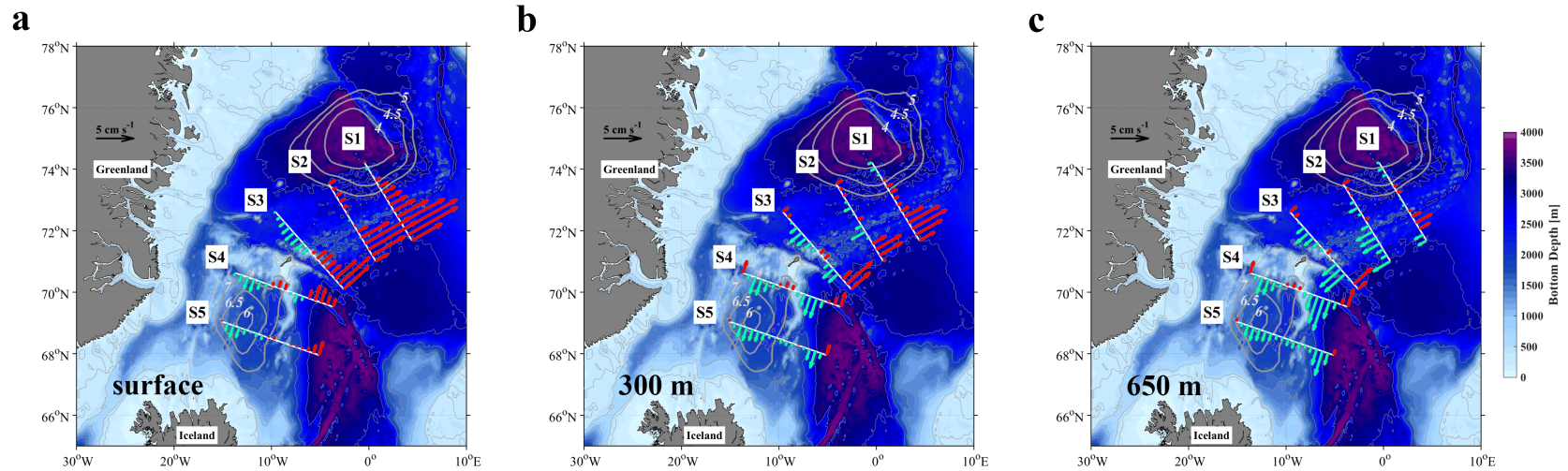
332
 333 **Figure 2| Proximity in water mass space to the densest overflow water.**
 334 **(a)** Distribution of the small potential density – potential spicity ($\sigma_0 - \pi_0$) distances ($\leq 0.05 \text{ kg m}^{-3}$)
 335 for late-winter (February-April) mixed layers from 2005 to 2015. Distances $> 0.05 \text{ kg m}^{-3}$ are
 336 shown by light-grey circles. The Greenland Sea and Iceland Sea gyres are delimited by the 4.5 and
 337 7 dynamic cm contours, respectively, of sea surface dynamic height relative to 500 db (thick black
 338 contours). The thin grey contours show the bathymetry from ETOPO2, with four ridges labeled:
 339 MR, Mohn Ridge; W-JMR, West Jan Mayen Ridge; JMR, Jan Mayen Ridge; KR, Kolbeinsey
 340 Ridge. **(b and c)** The year-round distribution of small $\sigma_0 - \pi_0$ distances in the 250-300 m layer and
 341 600-650 m layer, from 2005 to 2015. **(d)** The shallowest depth at which a small $\sigma_0 - \pi_0$ distance
 342 value (0.05 kg m^{-3}) is first found in the vertical. Stations where this value is not attained are shown
 343 by light-grey circles.



344

345 **Figure 3| Cross-pathway sections of potential temperature and potential density.**

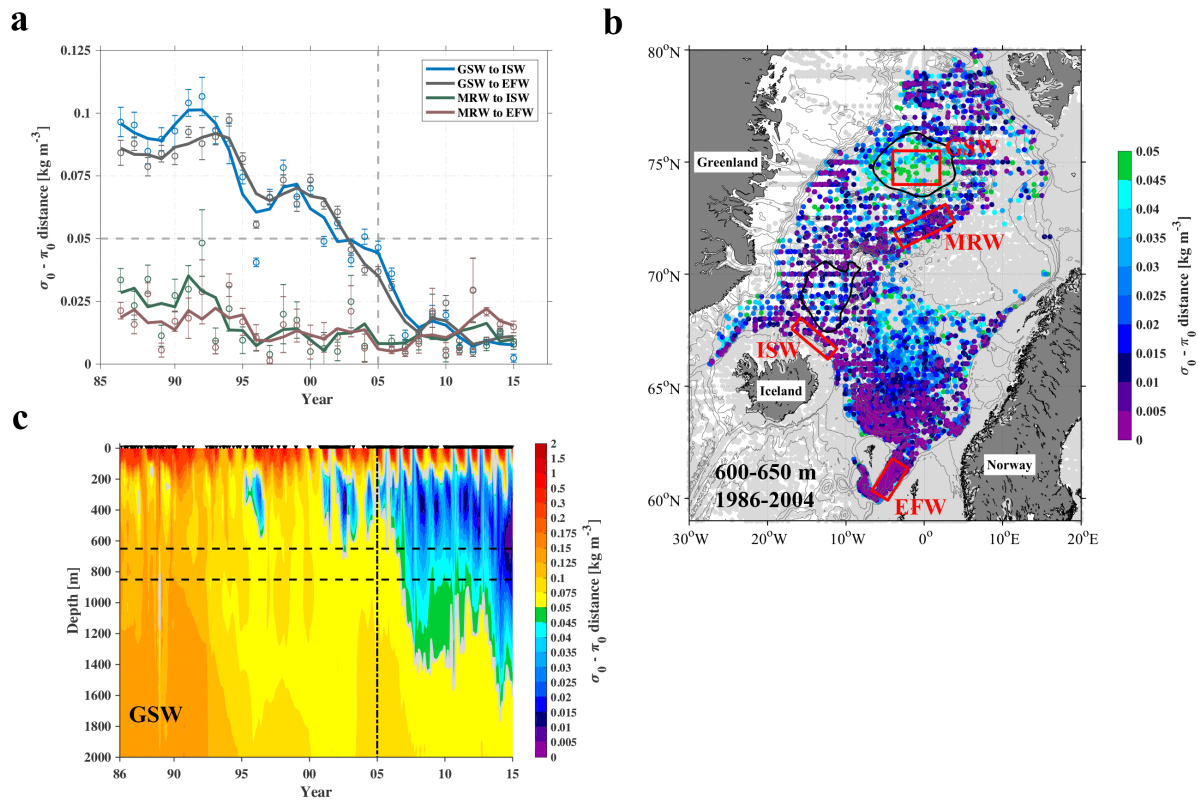
346 **(a)** Locations of the five composite sections (S1-S5) centered on the Mohn Ridge (MR) and Jan
 347 Mayen Ridge (JMR). The original and projected locations of hydrographic profiles used in each
 348 section are indicated by grey and black crosses, respectively. The red crosses denote the segment
 349 of the section used for calculating the absolute geostrophic velocity in Figure 4. The Greenland
 350 Sea and Iceland Sea gyres are outlined by the white contours. **(b)** The long-term mean (2005-2015)
 351 surface geostrophic velocity from the gridded satellite altimeter product. The two branches of the
 352 Norwegian Atlantic Current (NAC), the East Greenland Current (EGC), and the North Icelandic
 353 Irminger Current (NIIC) are labeled. The color indicates speed [cm s^{-1}]. **(c-g)** Cross-sections of
 354 potential temperature [$^{\circ}\text{C}$], overlain by potential density contours [kg m^{-3}]. The origin of the x axis
 355 in S1-S3 and in S4-S5 are the locations of Mohn Ridge and Jan Mayen Ridge, respectively. The
 356 horizontal dashed back line indicates the sill depth of Denmark Strait (650 m).



357

358 **Figure 4| Velocities along the pathways.**

359 Absolute geostrophic velocity [cm s^{-1}] normal to the five composite sections for (a) the surface, (b) 300 m, and (c) and 650 m, calculated
 360 using the hydrographic data and the satellite-derived surface geostrophic velocity in Figure 3. The southward and northward flows in
 361 each section are shown in blue and red, respectively. The Greenland Sea and Iceland Sea gyres are indicated by contours of sea surface
 362 dynamic height relative to 500 db in units of dynamic cm (thick grey contours).



363

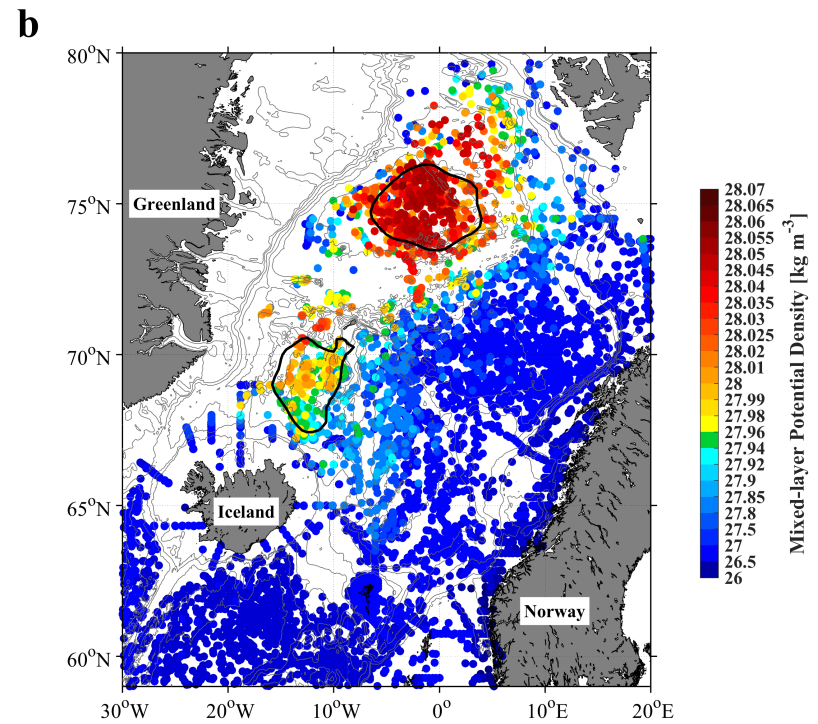
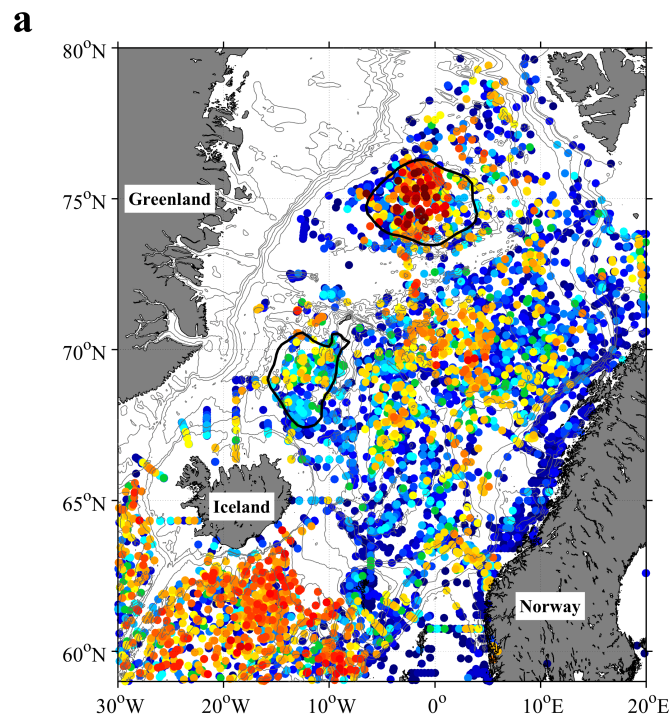
364 **Figure 5] Long-term variability of the densest overflow water.**

365 (a) Three-year running mean of $\sigma_0 - \pi_0$ distances between the densest overflow water ($28.03 \leq \sigma_0$
 366 $\leq 28.06 \text{ kg m}^{-3}$, $\theta \leq 0 \text{ }^\circ\text{C}$ and depth $\leq 850 \text{ m}$) in four geographical regions from 1986 to 2015:
 367 distance of GSW to ISW (blue solid line); GSW to EFW (grey solid line); MRW to ISW (green
 368 solid line); MRW to EFW (red solid line). The abbreviations are: Greenland Sea gyre water (GSW),
 369 Mohn Ridge water (MRW), North Iceland slope water (ISW), and East Faroes water (EFW). The
 370 four regions are outlined in Figure 5b. The solid circles are the annual means with error bars
 371 corresponding to the standard error. The vertical and horizontal dashed lines denote year 2005 and
 372 distance = 0.05 kg m^{-3} , respectively. (b) Distribution of the small $\sigma_0 - \pi_0$ distances between the
 373 time-varying NIJ transport mode and the water parcels in the 600-650 m layer, from 1986 to 2004.
 374 See text for details. (c) Evolution of $\sigma_0 - \pi_0$ distances between the time-varying NIJ transport mode
 375 and the water within upper 2000 m of the Greenland Sea gyre. The two horizontal dashed lines
 376 indicate the sill depths of Denmark Strait (650m) and the Faroe Bank Channel (850m). The vertical
 377 dashed line denotes year 2005. The grey contours denote $\sigma_0 - \pi_0$ distances = 0.05 kg m^{-3} .

378 **Supplementary Table 1 | Data sources with corresponding time periods and references.**

Data source	Years	Reference
UDASH (Unified Database for Arctic and Subarctic Hydrography)	1980-2015	<i>Behrendt et al., (2018)</i> https://doi.pangaea.de/10.1594/PANGAEA.872931
ICES (International Council for the Exploration of the Seas)	1980-2015	Data web page: http://ocean.ices.dk/HydChem/HydChem.aspx
WOD (World Ocean Database)	1980-2015	Data web page: www.noaa.gov/cgi-bin/OS5/SELECT/builder.pl
Argo float program	2001-2015	Data web page: https://doi.org/10.17882/42182
NISE (Norwegian Iceland Seas Experiment database)	1980-2009	<i>Nilsen et al., (2008)</i> , The NISE dataset, Faroese Fisheries Laboratory Tech. Rep. 08-01, 20pp
MFRI (Marine Freshwater and Research Institute of Iceland)	1980-2015	https://sjora.hafro.is
GLODAPv2 (Global Ocean Data Analysis Project version 2) - 2019	1980-2013	<i>Olsen et al., (2019)</i> https://doi.org/10.5194/essd-11-1437-2019 https://doi.org/10.25921/xnme-wr20

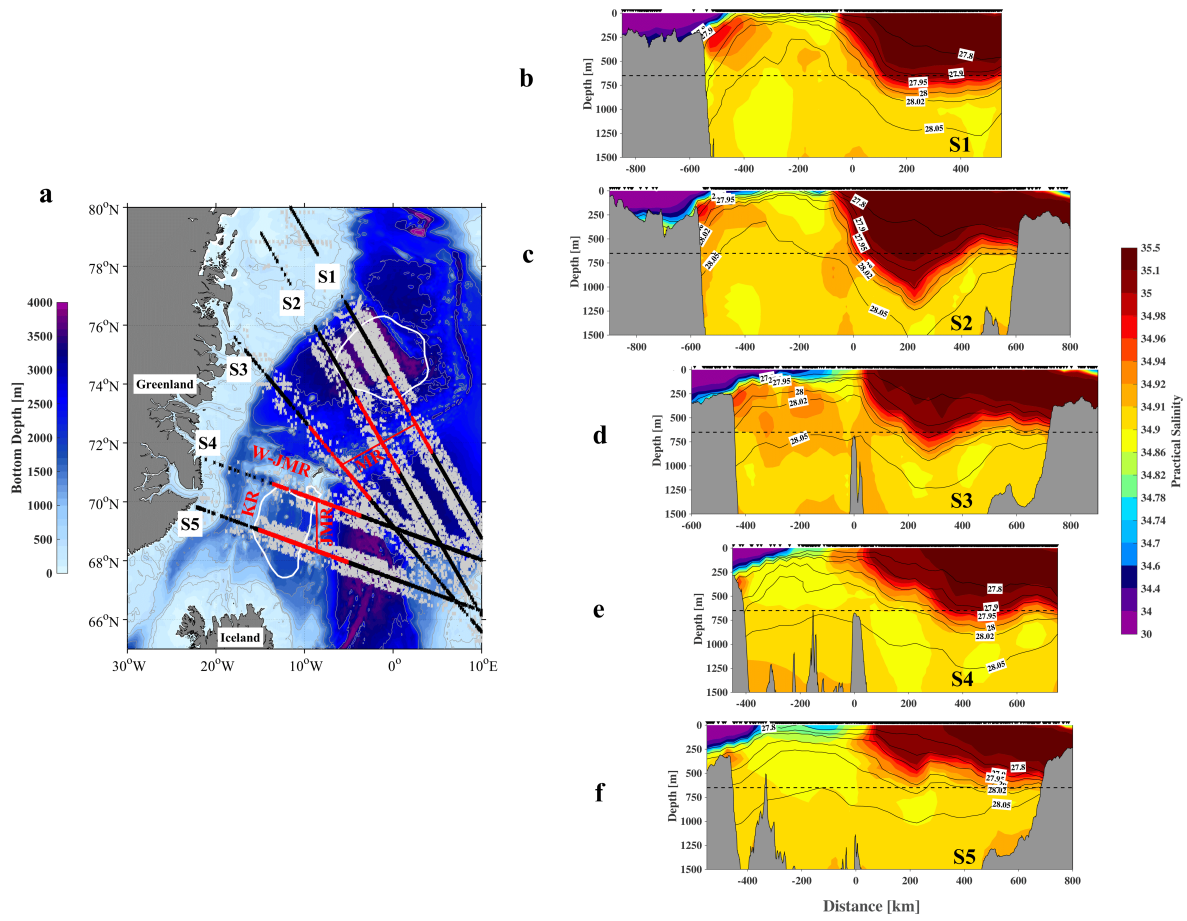
379



380

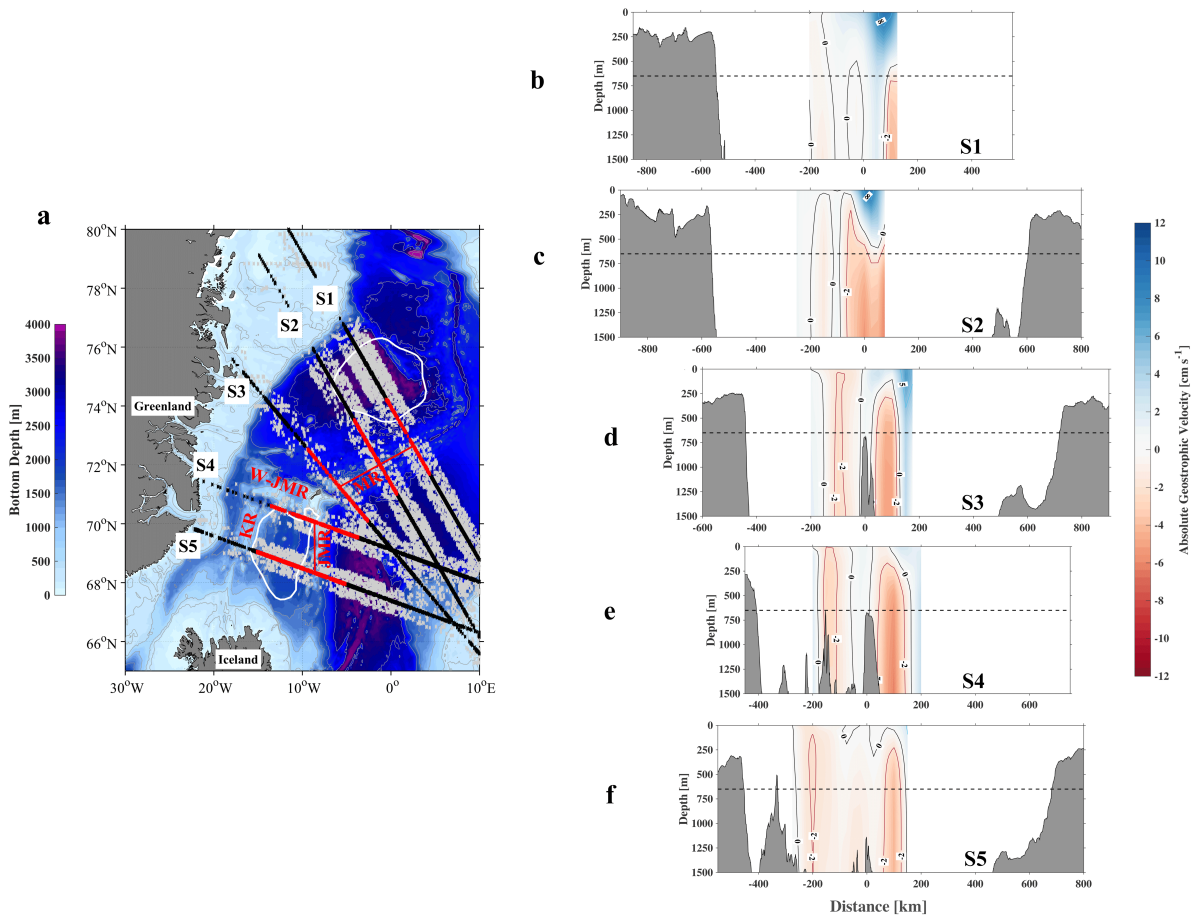
381 **Supplementary Figure 1 | Late-winter (February to April) mixed-layer properties.**

382 **(a)** Late-winter mixed-layer depth [m] and **(b)** mixed-layer potential density [kg m^{-3}]. The Greenland Sea and Iceland Sea gyres are
 383 outlined by thick black contours (see caption to Fig. 2). The thin grey contours show the bathymetry from ETOPO2.



384

385 **Supplementary Figure 2**| Same as Figure 3 except for salinity.



386

387 **Supplementary Figure 3**| Same as Figure 3 except for absolute geostrophic velocity.

388 Negative velocities are equatorward.